Journal of the Korean Nuclear Society
Volume 29, Number 1, pp. 85~91, February 1997

〈Technical Note〉

Flow-Induced Vibration Test in the Preheater Region of a Steam Generator Tube Bundle

Beom Shig Kim and Jong Keun Hwang
Korea Power Engineering Company, Inc.
150 Dukjin-dong, Yusong-gu, Taejon 305-353, Korea

(Received February 2, 1996)

Abstract

Cross-flow existing in a shell-and-tube steam generator can cause a tube to vibrate. There are four regions subjected to cross-flow in Yonggwang units 3 and 4 (YGN 3 and 4) steam generators, which are of the same design as the steam generators for Palo Verde nuclear power plant. Palo Verde units 1 and 2 steam generators have experienced localized wear at the corners of the cold side recirculating fluid inlet regions. A number of design modifications were made to preclude tube failure in specific regions of YGN 3 and 4 steam generators. Therefore, flow induced vibration experiments were done to determine the vibration magnitude of tubes in the economizer tube free lane region. The objective of this experiment is to demonstrate that the tube displacement is less than 0.01 inch rms at 100% of full power flow and to quantify the remaining design margin at 120% and 140% of full power flow.

1. Introduction

Cross-flow existing in a shell-and-tube steam generator can cause a tube to vibrate. In order to increase the component performance, higher flow velocities and reduced structural supports are required. However, these factors can lead to excessive flow induced vibration, which can cause tube failure by fretting-wear or by fatigue. It is essential to avoid such costly tube failures. This can be achieved by a thorough and comprehensive flow induced vibration evaluation at the design stage.

There are four regions subjected to cross-flow in Yonggwang units 3 and 4 (hereafter YGN 3 and 4) steam generators as shown in Fig. 1, which are of the same design as the steam generators for Palo Verde nuclear power plant. Palo Verde units 1 and 2 steam generators have experienced localized wear at the corners of the cold side recirculating fluid inlet region, which is located immediately above the economizer. It was concluded that the cause of the Palo Verde steam generator problem was excessive flow induced vibration caused by high fluid flow velocities at the edge of the economizer opening, along the tube free lane[1].

In order to preclude tube failure in specific regions of YGN 3 and 4 steam generators, a number of design modifications were made as follows : (1) raising the economizer divider plate to the top of the cold side recirculating fluid entrance window, (2) sealing the downcomer partitions, (3) extending the shroud circumferentially about seven inches at the cold side

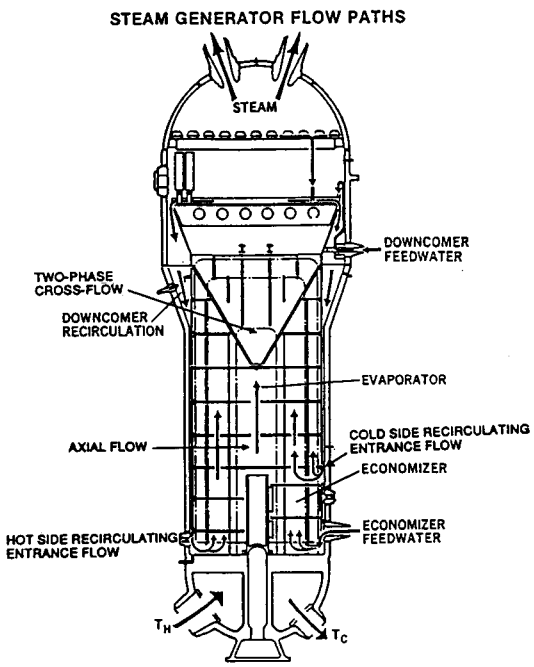

Fig. 1. Flow Pass in Tube Bundle of YGN 3 and 4 Steam Generator

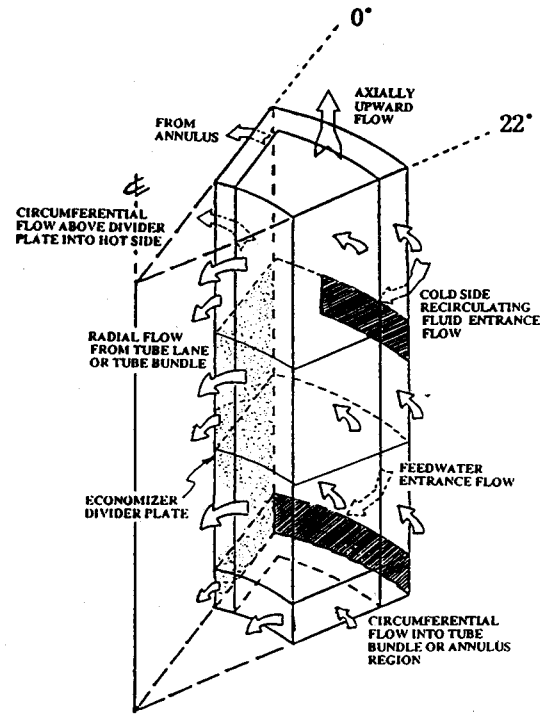

Fig. 2. Boundary Conditions of the Model Flow

recirculating flow entrance and (4) adding one additional "eggcrate" tube support in the economizer region.

In this paper, we present the results of flow induced vibration experiments done to determine the vibration magnitude of tubes in the economizer tube free lane region[2]. The objective of this experiment is to demonstrate that the tubes are not susceptible to harmful levels of vibration at 100% of full power flow and to quantify the remaining design margin at 120% and 140% of full power flow. The total flow through the test model is approximately $0.372 m^3/s$ for 100% of full power flow.

2. Flow Induced Vibration Experiment

The test model consists of a 22 degree sector of the cold leg of the steam generator. In this model, 0 degree corresponds to the centerline of the secondary side economizer divider plate as shown in Fig. 2. The 22 degree sector size is consistent with the analytical model of the steady state for thermal-hydraulic analysis of the steam generator. Figure2 shows the boundary conditions of the model flow. As shown in Fig. 2, there are seven circumferential flow region and two penetrations for feedwater and coldside recirculation water into the model. There are seven radial flow regions and two flow regions perpendicular to the economizer divider plate out of the model.

The test loop includes the storage tank, two pumps, the test model with piping connecting to the inlet and outlet plenum, associated valves, orifice plates and expansion joints. The loop was operated at atmospheric pressure and ambient temperature. The outer perimeter of the test model is of rectangular shape. This configuration was selected to simplify the test model construction assembly and alignment and to provide greater rigidity. The loop is normally operated at about 120°F and atmospheric pressure.

The test model contains 482 full size tubes with

165 made of Inconel 600 material (0.75″o.d. × 0.042″w.t.) and the remainder of Type 304 stainless steel. Figure3 shows a plan view of the model with flow inlet and outlet and selected tubes identified for monitoring. The stainless steel tubes were installed in non-critical flow regions to reduce the fabrication cost of the model. The Inconel tubes are located in Rows 1 through 7 adjacent to the tube lane and portions of nine lines along the circumferential outer tube boundary. The model depth, in the radial direction, is about 22 inches from the shroud. This is sufficient to evaluate tube vibration in a region encompassing the area of significant tube wear which occured in the Palo Verde steam generator. The distance between tubes or the pitch, p, was 1.0 inch, which gives p/d = 1.33. The configuration of tube bundle is the normal-triangular pattern(30degree).

The tubes were rolled into a 3 inch thick carbon steel tubesheet to provide constraint against rotational and translational motion. The tube length was about 220 inches. The tubes were laterally supported by one flow distribution plate and six typical tube supports as shown in Fig. 4. The tubes and supports extended vertically two levels above the downcomer recirculation entrance flow window. This is the region where the maximum annulus flow is predicted. Finite element model eigenvalue results indicate that the model extending two spans above the window is sufficient to obtain realistic vibration results.

The tube vibration response was measured with strain gages and accelerometers. Semiconductor strain gages were installed inside the tubes to provide reference measurements of the response to low frequency model motion. The tube response was measured at selected midspans or locations of greatest response for each test condition using movable biaxial accelerometers. These are spring-mounted devices designed for insertion into tubes. A total of 33 tubes were probed with the traversing accelerometer.

The tests were done at four test conditions simulating the flow rates predicted from the thermal-hydraulic analysis : 80%, 100%, 120% and 140% of full power flow. The total flow through the test model is approximately 0.372 m^3/s for 100% of full power flow.

The acceptance criteria for this test is 0.01 inch rms tube displacement at 100% of full power flow. The clearance between tube and tube supports was nominal 0.0125 inch. It generally corresponds to a vibration level that could cause tube damage such as

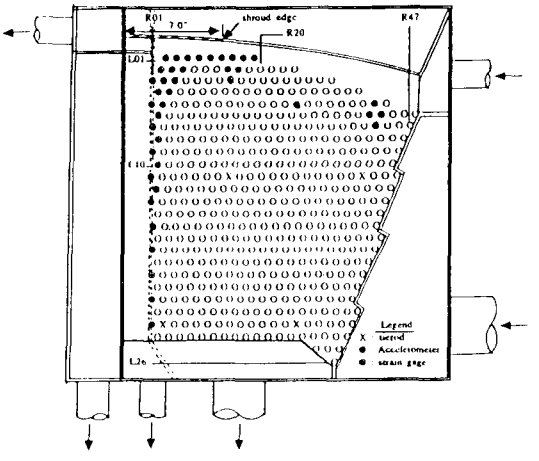

Fig. 3. Plan View of the Model Showing the Inlet and Outlet, and the Location of the Instrumentation

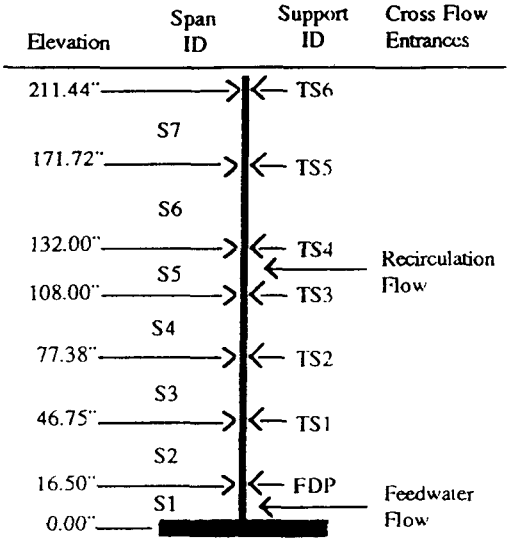

Fig. 4. Test Model : Typical Tube Support Geometry

fretting or wear[3].

3. Similitude Relations for Model Test

In order to get meaningful results, it is necessary to check the similarity of the test model to the prototype steam generator. In case of testing related to fluid-structure interaction this requires that geometric arrangement, magnitude and direction of fluid flow, and dynamic response of the structure be similar.

The tube vibration amplitude is a function of the following parameters.

$$X = F(L,\ p,\ d,\ \nu,\ \rho,\ V,\ \zeta,\ \lambda^2 K,\ M) \quad (1)$$

where L : characteristic tube length
p : tube pitch
d : tube diameter
ν : kinematic viscosity of fluid
ρ : fluid density
V : characteristic fluid velocity
ζ : damping ratio
$\lambda^2 K$: structural stiffness
M : mass per unit length.

These parameters describe the amplitude response of a tube in tube bundle subjected to cross-flow.

Equation (1) can be written in terms of dimensionless parameters as follows.

$$\frac{X}{d} = F\left[\ \frac{L}{d},\ \frac{p}{d},\ R_e, \zeta,\ \frac{\lambda^2 K}{\rho V^2 L},\ \frac{M}{\rho d^2}\ \right] \quad (2)$$

In equation (2), R_e is the Reynolds number, $\frac{\lambda^2 K}{\rho V^2 L}$ is the ratio of structural stiffness to dynamic loading, and $\frac{M}{\rho d^2}$ is the ratio of tube to fluid mass displaced.

The tubes and the tube supports for the model were installed using the same sizes as those of the prototype. The Reynolds number variation between test model and prototype is insignificant with regard to fluid forces acting on the tubes. The fluid forces are only weakly dependent on Reynolds number under all test flow conditions[4]. The fluid temperature is the main condition that is different between the model and the prototype, which is approximately 48°C(120°F) and 276°C(530°F), respectively. It is related to the variation of the fluid density. Therefore, we should consider the effect of temperature on damping and on the dynamic pressure. In liquids, viscous damping is one of the most important energy dissipation mechanisms for heat exchanger tubes. It might be slightly different due to temperature differences[5]. However, considering that the largest contribution to total tube damping results from the interaction between the tubes and the tube support, the similitude exists for total damping between the test model and the prototype. In order to maintain flow distribution similitude, the quantity ρV^2 for the model and the prototype steam generator has to be the same:

$$\rho_{sg} \cdot V_{sg}^2 = \rho_{model} \cdot V_{model}^2$$

$$V_{model} = V_{sg} \cdot \left[\ \frac{\rho_{sg}}{\rho_{model}}\ \right]^{1/2} \quad (3)$$

For the case of a fluid temperature of 48°C(120°F) for the model, $V_{model} = 0.863 V_{sg}$. This factor was considered to scale the flow rates for each entrance and exit of the model.

4. Results and Discussions

Fig. 5 is a plot of typical accelerometer output showing random orbital motion of the tube. The analysis results using the ANSYS code indicated that the lowest tube transverse vibration model would occur at around 33 Hz. Therefore, the tube vibration response was measured with an accelerometer and strain gages through a highpass filter set at 20 Hz to eliminate the low frequency of the structure/component.

The tube vibration response was measured at 80, 100, 120, and 140% of full power flow. Fig. 6 is a typical plot showing the power spectral density(PSD) for all four test conditions. There were several main peaks in the range of 20 Hz to 100 Hz, even though

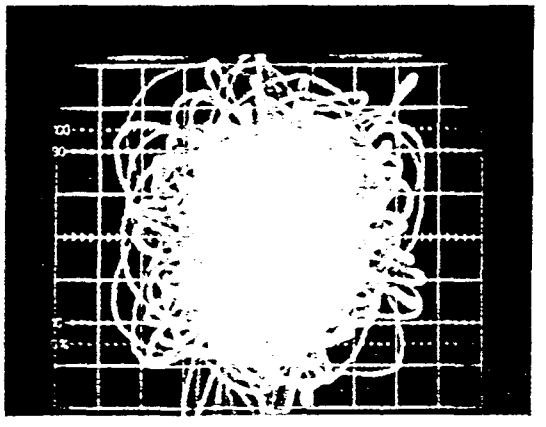

Fig. 5. Typical Random Orbital Tube Motion

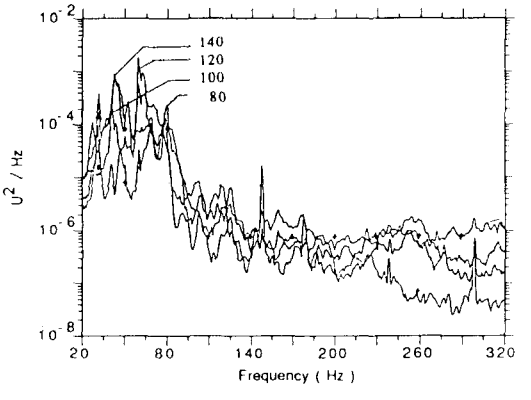

Fig. 6. Four PSD Plots at Different Design Flow

the adjacent peaks were very closely coupled to each other. However, there were no dominant peaks in the region of above 100 Hz.

Table 1 compares the calculated test model frequencies with those measured during testing. The hydrodynamic mass should be considered to calculate the natural frequency of tubes submerged in a fluid. The frequency range for the test model in Table 1 was obtained using a maximum hydrodynamic mass coefficient of 3.1 and an average value of 1.7 [6]. The results of frequencies calculated for the test model using the ANSYS code are generally in good agreement with those measured during the experiment.

Table 1. Frequency Comparisons Between ANSYS Calculated Measured Values

Mode No.	ANSYS Calculated Values* (Hz)	Measurd Values (Hz)
1	32.7~38.8	42
2	50.9~60.5	51
3	58.9~69.9	62, 72
4	77.8~92.4	80
5	99.9~118	103, 119
6	117.0~139.0	128
7	132~157.3	140, 158

* This range of frequencies was obtained using a maximum hydrodynamic mass coefficients of 3.1 and an average of the minimum and maximum values of 1.7, given in Ref. 6.

The largest displacement occured at the 140% of full power flow at the midspan of span 3 for tube R11−L1 and was about 0.88×10^{-3} inch rms, which is well below the test acceptance criteria of 0.01 inch. The displacement for 100% and 120% of full power flow was 0.34×10^{-3} inch rms and 0.53×10^{-3} inch rms, respectively, at the same location. The displacement of the adjacent tube, R13−L1, was about the 0.80×10^{-3} inch rms. The R11−L1 and the R13−L1 tubes are located near the edge of the shroud which has been extended circumferentially about 7 inches as one of the design modifications. This area is in the highly turbulent region where the downcomer fluid enters the window in the shroud and makes a 90 degree turn to travel circumferentially toward the tube free lane. The tube free lane corresponds to the region that experienced wear damage in Palo Verde steam generators. The width of the tube free lane between the economizer divider plate and the outer tube was increased from 0.81 inch to 1.31 inch. This decreased the fluid drag force and resulted in lowering the displacement of the tubes located near the tube free lane. Figure7 is a typical tube displacement at several tube elevations for test flow rates.

The displacements of each tube at the midspan

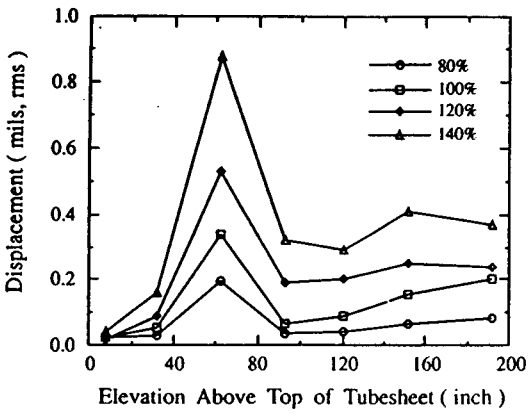

Fig. 7. Typical Tube Displacement According to Elevation

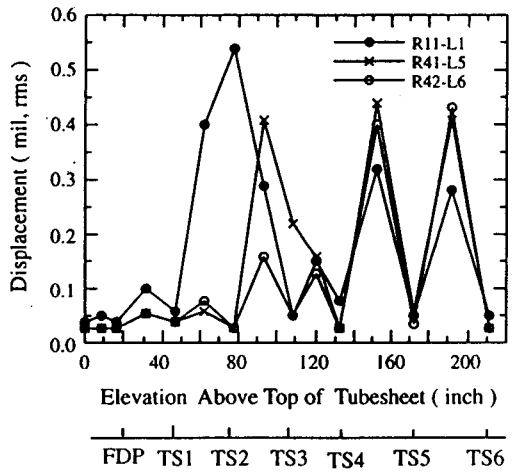

Fig. 8. Full Traversal Displacement of Three Tubes at 120% Design Flow

were generally greater than those at the tube supports as shown in Fig. 8, which is a typical tube displacement at each quarter span and tube support location. However, the displacements at tube support number 2 were greater than the adjacent midspan deflection, thereby indicating an ineffective tube support. This is based on the initial boundary condition of the tube within tube support.

Tube damping values were measured in air and in flow. Damping in air was measured at the midspan on span 3, 4, 5 and 6 of several tubes using the log-

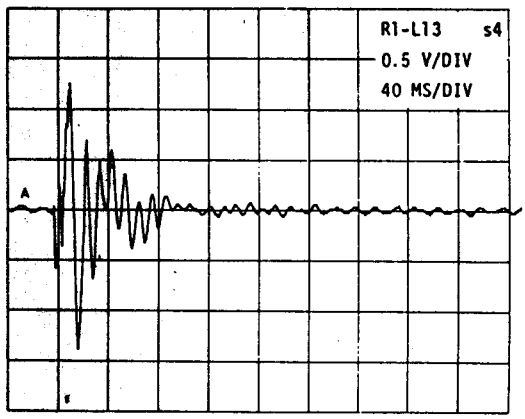

Fig. 9. Typical Logarithmic Decrement Trace in Air

Table 2. Tube Damping Data in Air

Tube Location	Damping Values at Midspan Position (%)			
	Span 3	Span 4	Span 5	Span 6
R1-L3	2.32	3.52	3.14	3.77
R1-L5	4.54	2.79	3.18	2.30
R1-L13	3.55	4.94	5.97	4.67
R1-L21	3.89	4.41	4.22	4.28
R2-L12	3.16	3.16	4.76	4.18
R2-L14	5.13	3.97	4.59	2.61

arithmic decrement method. The tube was struck to produce an impulsive loading. Figure 9 is the typical logarithmic decrement trace in air. Several modes of vibration were present. The frequencies of the main modes fell under the range of 50~70Hz and 75~90Hz, which correspond to the third mode and the fourth mode respectively. Table 2 shows the tube damping values in air. The average tube damping values in air was 3.79%.

The damping in flow was obtained from the response spectrum using the half power point method. Fig. 10 shows the damping data for the multispan tube in flow. As shown in the figure, there was some scatter in the data. These are based on low level of vibration amplitude for most tubes, less than 1.0×10^{-3} inch rms because of the difficulties in measuring damping in flow. Generally, the damping data tak-

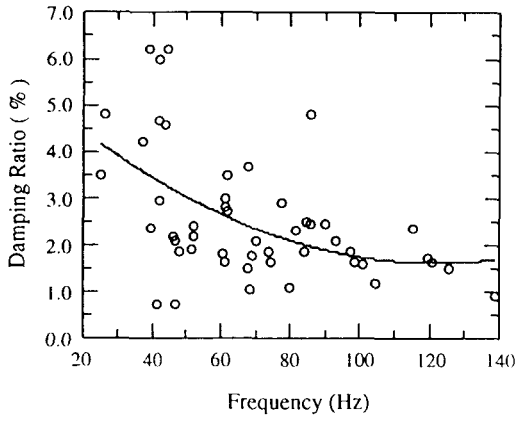

Fig. 10. Multispan Tube Damping in Flow

en from curve fitting decreased with tube frequency. A similar trend has been reported in the literature on heat exchange tube damping[7]. The range of tube damping was also reasonable.

5. Concluding Remarks

Experiments were done to measure the magnitude of tube vibration in the cold side economizer tube lane region of a steam generator. The following findings emerged from these experiments :

1) The tubes were not susceptible to harmful levels of vibration. The tube displacement for 100% power flow rate and 120% of full power flow was 0.34×10^{-3} inch rms and 0.53×10^{-3} inch rms, respectively, which is significantly less than the acceptance criteria of 0.01 inch rms.
2) The largest displacement for 140% of full power flow was 0.88×10^{-3} inch rms. This demonstrates that the tubes have significant design margin.
3) A number of design modifications contributed to decrease the level of tube vibration due to the flow velocity.

References

1. W.J. Heilker, N.L. Beard, and J.Y. Park, Flow Induced Vibration Analysis in Support of the design of the Yonggwang Units 3 and 4 Steam Generator, Proceedings of the International Symposium on Pressure Vessel Technology and Nuclear Codes and Standards, pp. 2-38~2-56, Seoul (1989)
2. N.L. Beard, D.E. Hart, J.K. Hayes, and W.J. Heilker, "Test Specification Flow Induced Tube Vibration Test Yonggwang Nuclear 3 and 4 Steam Generator Economizer and Lower Tube Bundle", ABB-CE Report CENC-1901, Revision 3 (1991)
3. M.J. Petigrew, and D.J. Gorman, "Vibration of Heat Exchanger Components in Liquid and Two-Phase Cross-Flow", Atomic Energy of Canada Limited Report AECL-6184 (1978)
4. B.T. Lubin, P.K. Shah, and J.G. Thakkar, "A Comparison of Degraded Tube Support Vibration Test Model Parameters Versus Millstone II Steam Generator", Combustion Engineering Report CENC-1785, Revision 3 (1988)
5. M.J. Pettigrew, C.E. Taylor, and B.S. Kim, "Vibration of Tube Bundles in Two-Phase Cross-Flow -Part 1 : Hydrodynamic Mass and Damping, "ASME Journal of Pressure Vessel Technology, Vol. 111, pp. 466-477 (1989)
6. S.S. Chen, and Ho. Chung, "Design Guide for Calculating Hydrodynamic Mass Part I : Circular Cylinderical Structures", Argonne National Laboratory, Technical Memorandum, ANL-CT-76-45 (1976)
7. M.J. Pettigrew, R.J. Rogers, and F. Axisa, "Damping of Multispan Heat Exchanger Tubes : Part 2;In Liquids", ASME PVP-Vol. 104 (1986)